

# Process optimization of corn starch nanoparticles containing linalyl acetate: characterization and antibacterial properties

Milad Gholami<sup>1</sup>, Morteza Hosseini<sup>1\*</sup>, Mohammad Hassan Shahavi<sup>2\*</sup>,  
Mohsen Jahanshahi<sup>1</sup>

<sup>1</sup>Department of Chemical Engineering, Babol Noshirvani University of Technology, Babol, Iran.

<sup>2</sup>Department of Nanotechnology, Faculty of Engineering Modern Technologies, Amol University of Special Modern Technologies (AUSMT), Amol, Iran.

\*Corresponding author: [m.hosseini@nit.ac.ir](mailto:m.hosseini@nit.ac.ir), [m.shahavi@ausmt.ac.ir](mailto:m.shahavi@ausmt.ac.ir)

## Original Research

## Abstract:

Received:  
22 March 2023  
Revised:  
1 September 2023  
Accepted:  
16 September 2023  
Published online:  
15 October 2023

In this research, the Taguchi approach optimized the preparation process of corn starch nanoparticles containing linalyl acetate (extracted from lavender). Sodium hydroxide and urea (solvent), ethanol (anti-solvent), and Tween 80 (surfactant) were employed for the synthesis in the nanoprecipitation method. The dimensions of the synthesized nanoparticles were measured by the dynamic light scattering method. The surface morphology of the nanoparticles was determined by atomic force microscopy and scanning electron microscopy. The results showed that the concentration of starch (2% w/w) and linalyl acetate (1.5% w/w), temperature (55° C), and the starch to the antisolvent ratio (1:15) had a significant effect on the size of the corn starch nanoparticle with the linalyl acetate. The predicted values for mean size, PDI, and zeta potential were 56.37 nm, 0.388, and -19.4 mV, respectively. Accordingly, the experimental values for mean size, PDI, and zeta potential were 59.7 nm, 0.395, and -22.7 mV, respectively. The size of the nanoparticles was 59.7 nm with a spherical shape under the optimum conditions. The optimal formula of nanoparticles' antibacterial properties against a gram-negative bacterial strain (*Escherichia coli*) and a gram-positive bacterial strain (*Staphylococcus aureus*) was evaluated. The maximum diameter of the inhibition zone determined by disk diffusion and well diffusion methods was 21 and 23 mm for *Staphylococcus aureus* and 16 and 18 mm for *Escherichia coli*. The minimum inhibitory concentration and minimum bactericidal concentration were observed at 12.5 mg/ml for *Escherichia coli* and 6.25 mg/ml for *Staphylococcus aureus*, which have a relatively good ability to inhibit these bacteria's growth.

**Keywords:** Antibacterial; Corn starch nanoparticles; Linalyl acetate; Nanoprecipitation; Taguchi

## 1. Introduction

Nowadays, the medicinal use of herbs and their extracts has become familiar again due to their extensive therapeutic properties and the improper use of chemicals in the manufacture of drugs. These herbs are a rich source of active pharmaceutical ingredients and primary and secondary metabolites [1, 2]. Applying synthetic drugs to infectious disease treatment may cause side effects, and these drugs are expensive. Therefore, it is necessary to develop novel

drugs for pathogenic microbial diseases and control their activities. One of the most abundant sources of medical ingredients (especially secondary metabolites) is plant species whose extracts could be utilized according to their therapeutic characteristics. These extracts are safe and effective in comparison with synthetic drugs [3, 4]. Herbal extracts as secondary metabolites contain hydrocarbons (terpenes and sesquiterpenes) and oxygenated compounds (alcohols, esters, ethers, aldehydes, ketones, and phenols) [5–7]. Pre-

**Table 1.** Factors and levels considered to produce CSLA<sub>NPs</sub>.

Parameters	Level 1	Level 2	Level 3
Starch concentration (%)	2	4	6
Linalyl acetate concentration (%)	1	1.5	2
Temperature (° C)	25	40	55
Starch to ethanol ratio (V:V)	1:5	1:15	1:25

vious studies have shown that some herbs used in food science have antibacterial effects [8–12]. The lavender extract contains compounds such as linalyl acetate (39.10%), linalool (29.7%),  $\alpha$ -terpinol (3.35%), trans-caryophyllene (3.76%), and other components (less than 1%), in which the active ingredient of lavender is linalyl acetate, classified as terpenes [13, 14].

Polysaccharide-based nanoparticles have been used to deliver hydrophilic drugs and preserve their physiological properties due to their unique properties [15–17]. Polysaccharides are stable, safe, non-toxic, hydrophilic, biodegradable compounds, abundant in nature, and inexpensive to process [18–21]. Polymeric nanoparticles have attracted much attention in drug delivery systems due to their controlled and slow-release, particle size smaller than a cell, biocompatibility, and increased therapeutic efficacy [22–27]. Starch is an abundant, inexpensive, non-toxic, and biodegradable biopolymer that can be used to synthesize polymeric nanoparticles through acid hydrolysis, extrusion, enzymatic hydrolysis, fluidized bed, precipitation, and the combination of acid hydrolysis and ultrasound [25–27].

Precipitation is a simple, attractive, and rapid method to produce nanoparticles from natural polymers [28]. The advantage of this method is the rapid formation of nanoparticles. Also, the whole process is carried out in a single step, requiring two solvents to dissolve each other, only one of which dissolves a polymer and drug [29, 30]. Corn starch contains protein (about 0.35%), fat and ash (0.8%), and two polysaccharides, amylose and amylopectin (98%) [31]. Nano-starch not only has no adverse effects on the environment or human health but could also be used to make a controlled and targeted release of drugs. Moreover, corn starch nanoparticles have a low gelatinization enthalpy. It can be used as a nanocarrier in coating and releasing bioactive compounds [32]. Linalyl acetate has been used as a precursor in the soap and flavoring industries for food and beverages, with biological properties such as antimicrobial, antioxidant, and anti-inflammatory properties [33]. Several researchers have previously tried to synthesize and optimize starch nanoparticles with different aims and aspects. For example, ethanol was selected as the best antisolvent to synthesize starch nanoparticles from dimethyl sulfoxide/corn starch solution [34–36]. Also, researchers used sodium hydroxide (solvent) and ethanol (antisolvent) to find that high-amylose starch is necessary to synthesize starch nanoparticles through the precipitation method [37]. There is no report on optimizing and preparing linalyl acetate-loaded starch nanoparticles in the literature, as per the authors' best knowledge. The antibacterial activity of linalyl acetate combined with the delivery characteristics of starch

nanoparticles could develop a novel biocompatible drug for anti-inflammatory applications. This research aimed to synthesize and optimize the size of corn-starch/linalyl-acetate nanoparticles (CSLA<sub>NPs</sub>) by the nanoprecipitation method and evaluate their antimicrobial activity. To optimize CSLA<sub>NPs</sub>, experiments were designed based on the Taguchi approach. The optimization was based on four different variables: starch concentration, linalyl acetate concentration, temperature, and starch solution to ethanol ratio. The effect of the optimization on the particle size distribution of the linalyl-loaded starch nanoparticles was evaluated. This approach was used to predict the significant contribution of parameters and the optimum combination of each parameter.

## 2. Materials and methods

Linalyl acetate (CAS Number: 115-95-7), sodium hydroxide (CAS Number: 1310-73-2), urea (CAS Number: 57-13-6), ethanol (CAS Number: 64-17-5), and tween 80 (CAS Number: 9005-65-6) were purchased from Merck (Darmstadt, Germany), and corn starch (CAS Number: 9005258) was purchased from Sigma-Aldrich (Steinheim, Germany) and used as received. Double-distilled water was used in all steps.

### 2.1 Experimental design

In this research, a three-level design with four parameters was established for experimental design. These factors include corn starch concentration, linalyl acetate concentration, temperature, and starch in the antisolvent ratio (Table 1). Each factor was tested at three levels, resulting in a total of eighty-one experiments. Table 2 illustrates the independent variables and their levels to evaluate CSLA<sub>NPs</sub> using the Taguchi method. All the experiments were performed in triplicate. The Minitab 18 statistical software and the Taguchi method were used to design the experiments. A value of  $p < 0.05$  was considered to be significant.

### 2.2 Preparation of nanoparticles containing lavender extract (linalyl acetate)

The particle size in each experiment with three replicates was analyzed as a response according to Table 1. Different concentrations of starch solution (2, 4, and 6%) were added (1:2) dropwise to the solution of sodium hydroxide (1 M) and urea (1 M). The mixture was stirred for 45 minutes at the desired temperatures (25, 40, and 55° C). Linalyl acetate with various concentrations (1, 1.5, and 2%) was added dropwise to the solution, and Tween 80 was used as a surfactant. The mixture was added to ethanol to obtain precipitate, centrifuged at 4500 rpm for 30 minutes, and

**Table 2.** Independent variables and their levels to evaluate CSLA<sub>NPs</sub> using the Taguchi method.

Experiment	Starch concentration (%)	Linalyl acetate concentration (%)	Temperature (° C)	Starch solution to ethanol ratio (v:v)
1	2	1	25	1:5
2	2	1.5	40	1:15
3	2	2	55	1:25
4	4	1	40	1:25
5	4	1.5	55	1:5
6	4	2	25	1:15
7	6	1	55	1:15
8	6	1.5	25	1:25
9	6	2	40	1:5

washed three times with pure ethanol [38]. The obtained precipitate was dried at ambient temperature and used for the following experiments.

### 2.3 Morphological characterization of CSLA<sub>NPs</sub>

The surface morphology of CSLA<sub>NPs</sub> was analyzed using a field emission scanning electron microscope (FE-SEM, MIRA3, TESCAN, Czech Republic). The dried and powdered precipitate was placed on the SEM base and coated with a layer of gold to improve image resolution. An atomic force microscope (AFM, Nanosurf EasyScan2® Flex, Switzerland) was employed for characterizing the size distributions of nanoparticles to evaluate two-dimensional and three-dimensional particle shape and size. Moreover, the dried sample (1 mg) was dissolved in distilled water (10 mL) and dispersed in an ultrasonic apparatus for 1 minute, and the nanoparticle dimensions and zeta potential were analyzed through the dynamic light scattering (DLS) method using the HORIBA SZ-100 nanoparticle analyzer (Horiba, Kyoto, Japan).

### 2.4 Bacterial culture

*Escherichia coli* (*E. coli* PTCC1399) and *Staphylococcus aureus* (*S. aureus* PTCC1431) were obtained from Iran's Pasteur Institute. The bacteria used were cultured on Mueller Hinton Agar medium in an incubator at the desired temperature and moisture.

### 2.5 Evaluation of antibacterial properties of CSLA<sub>NPs</sub>

#### 2.5.1 The disk diffusion method

The Kirby-Bauer disk diffusion test was used to evaluate the antibacterial effect of CSLA<sub>NPs</sub>. The disks containing various nanoparticles were prepared by adding 50  $\mu$ L of each nanoparticle (at a concentration of 100%) to sterile blank disks and observing the absorption of nanoparticles in paper disks for 1 h. Then, disks were incubated in the bacterial culture plates at 37° C for 24 h. Experiments were carried out with three replications [39].

#### 2.5.2 The well-diffusion method

This method was used to evaluate the antibacterial effects of CSLA<sub>NPs</sub>. Plates containing the Mueller Hinton Agar medium and microorganisms were used for this purpose. A hole was cut in the culture medium and filled with the

extract (50  $\mu$ L with 100% concentration). After 24 hours of incubation at 37° C for the plates, the diameter of the zone of inhibition (mm) was determined.

### 2.5.3 Determination of minimum inhibitory concentration (MIC) and minimum bactericidal concentration (MBC) by the micro-broth dilution method

First, bacterial suspensions (20  $\mu$ L) were seeded in a 96-well plate containing the Mueller Hinton Agar medium (150  $\mu$ L). Then, 200  $\mu$ L of different concentrations of CSLA<sub>NPs</sub> (100%, 50%, 25%, 12%, and 6.25%) were added to each well. Each well containing the medium, bacterial suspension, and antibiotic (50  $\mu$ L) was considered a positive control. Moreover, each well containing the medium and bacterial suspension was used as the negative control. This plate was incubated at 37° C for 24 h. After the incubation, each row of wells with a special concentration of CSLA<sub>NPs</sub> in the plate was assessed, and the first concentration of CSLA<sub>NPs</sub> with no red color was considered minimum inhibitory concentration (MIC), and the first concentration with no growth was minimum bactericidal concentration (MBC) [40, 41].

## 3. Results and discussion

### 3.1 Optimization

In this research, the CSLA<sub>NPs</sub> synthesis process was optimized to produce nanoparticles with the smallest size. The results (Fig. 1) showed that the experiment with a starch concentration of 20 mg/mL, a linalyl acetate concentration of 15 mg/mL, a temperature of 55° C, and a starch to ethanol ratio of 1:15 (v/v) led to the smallest particle size (56.37 nm).

S/N graphs in Fig. 1(a–c). display the mean value of the S/N ratio in decibels (dB) at various process parameter levels for zeta potential (mV), PDI, and mean droplet size (nm). According to the results, the smaller S/N ratio was the higher-quality feature of nanoprecipitation.

In the Taguchi method, the effectiveness of each variable can be expressed by S/N. The N is the noise factor, indicating the difficulty of controlling the quantity, and the S is called the signal factor, indicating simple control of the variable [42]. The optimal conditions and how they affected the size of the synthesized CSLA<sub>NPs</sub> were ascertained using the Taguchi method. In this method, the S/N ratio with a higher value indicates smaller nanoparticles synthesized.

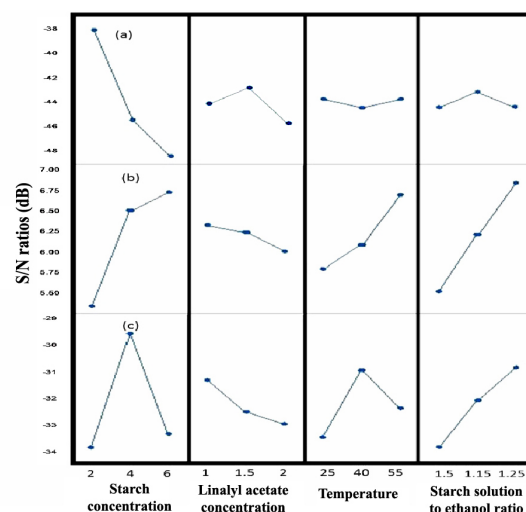
**Table 3.** ANOVA for (a) mean droplet size (nm), (b) PDI, and (c) zeta potential (mV).

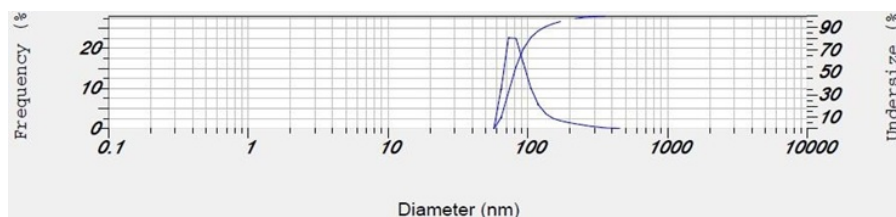
Factors	DOF(F)	Sum of Squares(SS)	Variance(V)	F-ratio(F)	Percent P (%)
<b>(a) Size (nm)</b>					
Starch Concentration (wt%)	2	127387.624	63693.812	10168.714	58.24
Linalyl acetate concentration(wt%)	2	2711.044	1355.522	216.409	1.87
Temperature (° C)	2	131.745	65.873	10.517	0.08
Starch Solution to ethanol ratio(V/V)	2	5399.167	2699.584	430.988	33.73
Error	18	112.747	6.264		6.08
Total	26	144353.194			100
<b>(b) Zeta Potetial</b>					
Starch Concentration (wt%)	2	996.361	498.180	655.181	38.06
Linalyl acetate concentration(wt%)	2	161.512	80.756	106.206	6.12
Temperature (° C)	2	748.022	374.011	491.880	28.56
Starch Solution to ethanol ratio(V/V)	2	607.470	303.735	399.456	23.18
Error	18	13.687	0.760		4.08
Total	27	2613.663			100
<b>(c) PDI</b>					
Starch Concentration (wt%)	2	0.005	0.002	4.875	34.71
Linalyl acetate concentration(wt%)	2	0.008	0.004	8.340	11.30
Temperature (° C)	2	0.008	0.004	7.776	23.98
Starch Solution to ethanol ratio(V/V)	2	0.009	0.004	8.716	22.33
Error	18	0.009	0.000		7.68
Total	26	0.039			100

Fig. 1 shows the value of the S/N ratio for the CSLA<sub>NPs</sub> synthesized by the nanoprecipitation method. The S/N ratio was achieved using Equation 1, and the data show that the S/N ratio with a higher value results in smaller particle sizes [43, 44].

Using ANOVA, the goal is to find out which process parameter most significantly affects the characteristics of starch nanoparticles, such as their lowest PDI and mean diameter under 59.7 nm, with a zeta potential below -30 mV (high

stability). The ANOVA for (a) mean droplet size (nm), (b) PDI, and (c) zeta potential (mV) is presented in Table 3. The rows in this table labeled “Error” indicate the experimental error as well as the errors brought on by uncontrollable factors (noise) that were excluded from the experiment. The results would not be trustworthy if the value was greater than 50% on average. The mean droplet size experiments, zeta potential experiments, and PDI experiments had calculated errors of 6%, 4%, and 7.7%, respectively. It is obvious

**Figure 1.** S/N ratio graphs for (a) mean size (nm), (b) PDI, and (c) zeta potential (mV).



**Figure 2.** Analysis of dynamic light scattering from the optimized CSLANPs with an electric current intensity of 1 A.

that they are below the limit. The negligible errors of the experiments suggest that almost all essential and effective factors were taken into account.

The predicted S/N ratios under ideal circumstances for zeta potential -temperature at level 2, linalyl acetate concentration at level 1, concentration of starch concentration at level 2, and starch solution to ethanol ratio (V:V) at level 3- was about -19.4 mV (Table 4 part c). The experimental values were fairly close to the predicted values when compared to the data from the final optimization step and the Taguchi method. According to the obtained data, the starch concentration was identified as another effective parameter for PDI, zeta potential, and particle size of nanoparticles.

Estimating process performance under ideal conditions can be done using ANOVA. Conditions that can lead to the smallest S/N ratio are considered optimal in the Taguchi method. Levels that indicate the ideal circumstances for a factor under consideration have a low S/N ratio. The process parameter for the ideal properties of starch nanoparticles differs according to the ANOVA results. Table 4 represents the results of optimum conditions for mean size, PDI, and zeta potential. Also, the minimum particle size was determined by the S/N ratio at both the optimal and expected conditions. The expected values for zeta potential, mean size, and PDI were -19.4 mV and 56.37 nm, respectively. As a result, the experimental values for zeta potential, mean size, and PDI were, respectively, -22.7 mV and 59.7 nm.

$$\frac{S}{N} = -10 \log \frac{(\frac{1}{y_1^2} + \frac{1}{y_2^2} + \dots + \frac{1}{y_n^2})}{n} \quad (1)$$

In other words, the optimum conditions of the parameters are at level 1 for the corn starch concentration, level 2 for linalyl acetate concentration, level 3 for temperature, and level 2 for starch to ethanol ratio.

The optimal conditions and the influence of different parameters on the size of CSLANPs can be predicted by Equation 2. An ANOVA test was used to analyze the results and

determine the effect of each parameter [45].

$$Y = \frac{T}{N} + (C - \frac{T}{N}) + (S - \frac{T}{N}) + (t - \frac{T}{N}) + (E - \frac{T}{N}) \quad (2)$$

Where Y is the estimated value of nanoparticle size under optimum conditions, T represents the sum of the results. N is the total number of experiments performed. Also, S, C, t, and E are the average results at optimum starch concentration levels, linalyl acetate concentration, temperature, and starch ratio to ethanol, respectively. The nanoparticles' size was estimated at 56.37 nm by Minitab software (Version 18) at optimum conditions. After repeating experiments with the prediction, the mean size of the nanoparticles was about 59.7 nm.

Equation 3 shows the significant effect of parameters A, B, C, and D on nanoparticles' size.

$$\text{Particle size} = 119.58 - 57.68A_1 - 4.74A_2 + 62.42A_3 + 21.22D_1 + 2.86D_2 - 24.08D \quad (3)$$

where A, B, C, and D are the starch concentration, linalyl acetate concentration, temperature, and starch-to-ethanol ratio factors, respectively. NaOH and urea, as inexpensive and non-toxic solvents, are used in this research to improve the solubility of corn starch. This effect depends on the ratio of NaOH and urea concentrations. NaOH leads to the breaking of intermolecular and intramolecular hydrogen bonding in starch molecules. On the other hand, urea prevents the self-association of starch molecules [46]. The effect of starch concentration on the size of CSLANPs was also evaluated. A certain concentration of starch (20 mg/mL) was the best for the optimization. A higher concentration of starch and consequently denser molecular chains increase the solution's viscosity, leading to mass transfer resistance to diffusion of the solvent into the precipitate.

Moreover, the temperature is related to the swelling and gelatinizing of starch granules [38]. After dissolving corn starch nanoparticles in the solvent, they were precipitated

**Table 4.** Optimum conditions for mean droplet size, PDI, and zeta potential.

Factors	D(a) Mean Size (nm)		(b) PDI		(c) Zeta Potential (mV)	
	Level	Description	Level	Description	Level	Description
Starch Concentration (wt%)	1	2	3	6	2	4
Linalyl acetate concentration (wt%)	2	1.5	1	1	1	1
Temperature (° C)	3	55	3	55	2	40
Starch Solution to ethanol ratio (V:V)	2	1:15	3	1:25	3	1:25
Expected result at optimum condition		56.37		0.388		-19.4

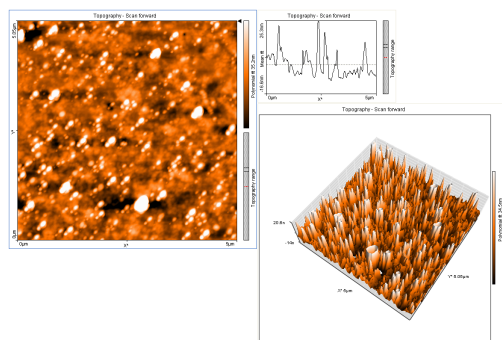


**Figure 3.** Analysis of surface morphology of CSLANPs using AFM.

by adding ethanol. The present study showed that a starch-to-ethanol ratio equal to 1:15 is the best ratio for optimizing corn starch nanoparticles with a spherical shape and a size of 59.7 nm. The surfactant (Tween 80) was used to limit the growth of starch nanoparticles.

### 3.2 Evaluation of dynamic light scattering (DLS)

According to the results obtained from the DLS experiment with an electrical current intensity of 1 A in deionized water under ultrasonic conditions (Fig. 2), the average particle size was determined to be about 60 nm dispersed in the solution in the range of 50 – 300 nm. The optimum conditions were selected to synthesize the particles for this evaluation. It has also demonstrated the highest percentage of particle size, about 60 nm, with a frequency of 80%. The results are in good correspondence with theoretical optimization data. From the optimization results, the optimum average size of the particles was predicted to be about 56.37 nm, which is close to the experimental evaluation results.

### 3.3 Analysis of AFM images

Fig. 3 shows the AFM image of the CSLANPs, which was synthesized in optimum conditions. The results illustrated the spherical shape of the particles. The particle size distribution of the synthesized CSLANPs, which is calculated from the image processing of the AFM image, is shown in Fig. 4. The particle size was in the range of 17 – 170 nm, and the highest frequency is about 30 – 70 nm, which confirms the results obtained from the DLS analysis and optimization estimation.

### 3.4 FE-SEM images

The results of FE-SEM images are shown in Fig. 5. According to the images, the size of starch granules as a control sample was in the range of 10 – 30  $\mu\text{m}$  (Fig. 5A), and the

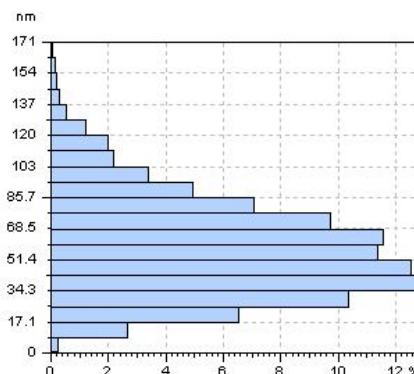


**Figure 4.** CSLANPs size distribution graph appeared by AFM microscope.

particle size in the range of 12 – 100 nm is obvious for the optimized CSLANPs (Fig. 5B).

The optimized CSLANPs average size estimation from the Taguchi method was 56.37 nm, which is confirmed by the results of FE-SEM images. The data are also in good correspondence with other reports in this field. According to a study by Xiao et al., the nanoparticle size of starch prepared by nanoprecipitation from broken rice was about 100 to 800 nm [47]. Another report by Qiu et al. represents menthone-loaded starch nanoparticles by the same method, with particle sizes ranging from 93 to 113 nm [48]. These differences in size can be related to the different starch granules' sizes from different sources [49].

### 3.5 Evaluating the antibacterial activity of CSLANPs

The antibacterial activity of CSLANPs was evaluated by disk diffusion and the “well diffusion method” against a gram-negative bacterial strain (*Escherichia coli*) and a gram-positive bacterial strain (*Staphylococcus aureus*). It was evident from the results that these nanoparticles could stop the growth of these bacteria quite effectively (shown in Table 5).

According to the results, the maximum diameter of the inhibition zone determined by disk diffusion and well diffusion methods was 21 and 23 mm for *Staphylococcus aureus* and 16 and 18 mm for *Escherichia coli*, respectively (Fig. 6).

Both the minimum bactericidal and minimum inhibitory concentrations were found at dilutions of 12.5 mg/ml for *Escherichia coli* and 6.25 mg/ml for *Staphylococcus aureus*, respectively (Fig. 7).

The inhibition method zone is a famous procedure to estimate the inhibitory effects of antimicrobial materials against specific bacterial strains. This assay is usually used to an-

**Table 5.** The antibacterial activity of CSLANPs was evaluated using disk diffusion and well diffusion and their MIC and MBC.

Species	Methods			
	Well diffusion (mm)	Disk diffusion (mm)	MIC concentration (mg/ml)	MBC concentration (mg/ml)
<i>S.aureus PTCC1431</i>	23	21	6.25	6.25
<i>E.coli PTCC1399</i>	18	16	12.5	12.5

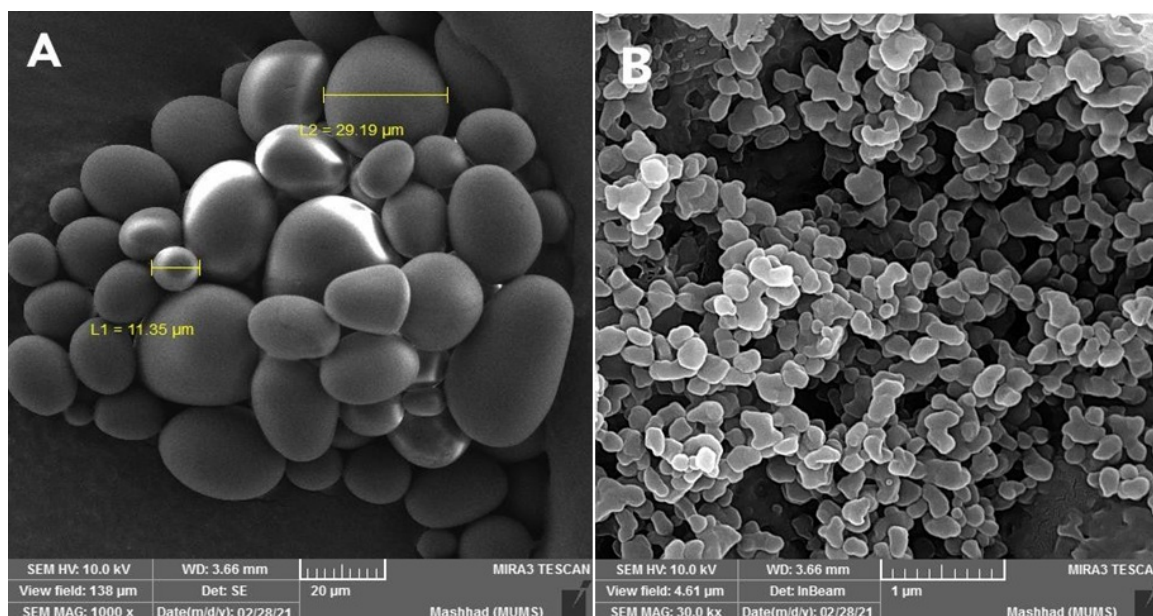


**Figure 5.** FE-SEM images: A: corn starch granules, HV 10 kV, magnification 1000X; B: optimized CSLA<sub>NPs</sub>, HV 10 kV, magnification 30000X.

alyze the antibacterial activity of materials with diffusible potential. As the material diffuses away from the disk, the concentration declines logarithmically. The antibacterial activity of the agent and sensitivity of the bacteria are judged by the appearance and size of a zone where no growth occurs, the zone of inhibition [50–52]. Ismail and Gopinath [53] loaded antibiotics on starch nanoparticles to evaluate their antibacterial activity. Their results showed that the highest antibiotic concentration (10 mg/ml) loaded led to an inhibition zone of 27 mm, indicating high antibacterial activity. Thus, the disk diffusion method’s results using lavender extract in the present study showed that the CSLA<sub>NPs</sub> had relatively good antibacterial activity.

### 4. Conclusion

The effect of four different parameters, including starch concentration, linalyl acetate concentration, temperature, and the ratio of starch solution to antisolvent, on the properties of corn starch nanoparticles and their microbial activity have been optimized. The Minitab software and Taguchi methods have been used to combine mathematical and statistical methods in experimental research. These methods suggested nine experiments to find the optimum particle size. The solvents used in this research play two different roles: (1) breaking the intermolecular and intramolecular hydrogen bonding in starch molecules, and (2) preventing the aggregation and linking of the broken starch molecules and increasing their solubility. An antisolvent is used for the separation and cleaning of

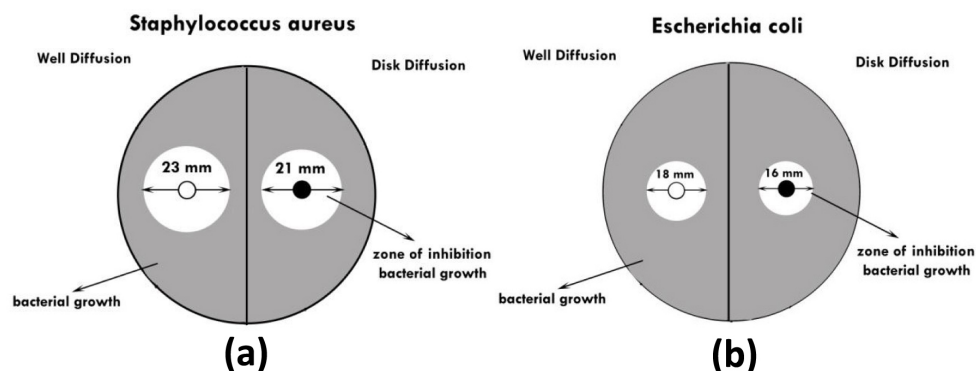


**Figure 6.** The antibacterial activity of CSLA<sub>NPs</sub> was evaluated using the disk diffusion method and the well diffusion method on (a) *S. aureus* PTCC 1431 and (b) *E. coli* PTCC 1399. The circle shows the inhibition zone.

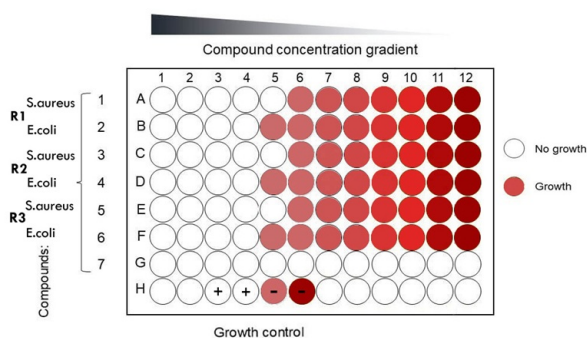


**Figure 7.** MIC and MBC testing of CSLA<sub>NPs</sub>: The positive sign (+) shows that the wells contain CSLA<sub>NPs</sub>, and the negative sign (-) shows the wells with no CSLA<sub>NPs</sub>.

the precipitated starch from the solvent. According to the experimental results suggested by the Taguchi method, the optimum conditions for the synthesis of the small starch nanoparticles are as follows: a temperature of 55° C, the corn starch concentration of 2% w/w, the linalyl acetate concentration of 1.5% w/w, and the starch solution to the antisolvent ratio of 1:15. It was also observed that the size of nanoparticles decreased by increasing the temperature and reducing the starch concentration. Analysis of dynamic light scattering showed that the average size of starch nanoparticles was about 60 nm. The results obtained from the SEM and AFM analyses also confirmed that the CSLANPs nanoparticles are spherical particles with a size distribution of about 12 – 100 nm. At the optimum condition, the size of nanoparticles was estimated to be 56.37 nm using the Minitab software. It can be concluded that the corn starch nanoparticles containing linalyl acetate have the potential to be used as nanomedicine. Moreover, these nanoparticles showed antibacterial activity against the gram-negative bacterial strain (*Escherichia coli*) and the gram-positive bacterial strain (*Staphylococcus aureus*); therefore, they can be an appropriate option for facilitating the healing of the scar.

#### Acknowledgment:

The data for this article was extracted from a Ph.D. dissertation in chemical engineering. The authors gratefully acknowledge the research laboratories of the Amol University of Special Modern Technologies (AUSMT).

#### Ethical approval:

This manuscript does not report on or involve the use of any animal or human data or tissue. So the ethical approval does not applicable.

#### Funding:

No funding was received to assist with conducting this study and the preparation of this manuscript.

#### Authors Contributions:

All authors have contributed equally to prepare the

paper.

#### Availability of data and materials:

The data that support the findings of this study are available on request from the corresponding author.

#### Conflict of Interests:

The authors declare that they have no known competing financial interests or personal relationships that could have appeared to influence the work reported in this paper.

#### Open Access

This article is licensed under a Creative Commons Attribution 4.0 International License, which permits use, sharing, adaptation, distribution and reproduction in any medium or format, as long as you give appropriate credit to the original author(s) and the source, provide a link to the Creative Commons license, and indicate if changes were made. The images or other third party material in this article are included in the article's Creative Commons license, unless indicated otherwise in a credit line to the material. If material is not included in the article's Creative Commons license and your intended use is not permitted by statutory regulation or exceeds the permitted use, you will need to obtain permission directly from the OICCPress publisher. To view a copy of this license, visit <http://creativecommons.org/licenses/by/4.0>.

#### References

- [1] A. Zeberli, S. Badr, C. Siegmund, M. Mattern, and H. Sugiyama. "Data-driven anomaly detection and diagnostics for changeover processes in biopharmaceutical drug product manufacturing." *Chemical Engineering Research and Design*, **167**:53–62, 2021. DOI: <https://doi.org/10.1016/j.cherd.2020.12.018>.
- [2] N. Targhazeh, R. J. Reiter, M. Rahimi, D. Qujeq, T. Yousefi, M. H. Shahavi, et al. "Oncostatic activities of melatonin: Roles in cell cycle, apoptosis, and autophagy." *Biochimie*, **200**:44–59, 2022. DOI: <https://doi.org/10.1016/j.biochi.2022.05.008>.
- [3] P. Agrawal, D. Kotagiri, and V. Kolluru. "Comparative analysis of antimicrobial activity of herbal extracts against pathogenic microbes." *Advances in Biochemistry and Biotechnology*, **10**:2574–8, 2018.
- [4] M. J. Firdhouse and P. Lalitha. "Flower-shaped gold nanoparticles synthesized using Kedrostis foetidissima and their antiproliferative activity against bone cancer cell lines." *International Journal of Industrial Chemistry*, **7**:347–58, 2016. DOI: <https://doi.org/10.1007/s40090-016-0098-4>.
- [5] R. Ben Mrid, B. Benmrid, J. Hafsa, H. Boukcim, M. Sobeh, and A. Yasri. "Secondary metabolites as



- biostimulant and bioprotectant agents: A review.”. *Science of The Total Environment*, **777**:146204, 2021. DOI: <https://doi.org/10.1016/j.scitotenv.2021.146204>.
- [6] M. Hassanpour, M. H. Shahavi, G. Heidari, A. Kumar, M. Nodehi, F. D. Moghaddam, et al. “Ionic liquid-mediated synthesis of metal nanostructures: Potential application in cancer diagnosis and therapy.”. *Journal of Ionic Liquids*, **2**:100033, 2022. DOI: <https://doi.org/10.1016/j.jil.2022.100033>.
- [7] B. Karakashov, S. Grigorakis, S. Loupassaki, I. Mourtzinis, and D. P. Makris. “Optimisation of organic solvent-free polyphenol extraction from *Hypericum triquetrifolium* Turra using Box–Behnken experimental design and kinetics.”. *International Journal of Industrial Chemistry*, **6**:85–92, 2015. DOI: <https://doi.org/10.1007/s40090-015-0034-z>.
- [8] N. Belarbi, F. Dergal, I. Chikhi, S. Merah, D. Lerari, and K. Bachari. “Study of anti-corrosion activity of Algerian *L. stoechas* oil on C38 carbon steel in 1 M HCl medium.”. *International Journal of Industrial Chemistry*, **9**:115–25, 2018. DOI: <https://doi.org/10.1007/s40090-018-0143-6>.
- [9] M. R. Youssefi, R. Alipour, Z. Fakouri, M. H. Shahavi, N. T. Nasrabadi, M. A. Tabari, et al. “Dietary supplementation with eugenol nanoemulsion alleviates the negative effects of experimental coccidiosis on broiler chicken’s health and Growth performance.”. *Molecules*, **28**:2200, 2023.
- [10] M. Azizkhani, F. Jafari Kiasari, F. Tooryan, M. H. Shahavi, and R. Partovi. “Preparation and evaluation of food-grade nanoemulsion of tarragon (*Artemisia dracunculoides* L.) essential oil: antioxidant and antibacterial properties.”. *Journal of Food Science and Technology*, **58**:1341–8, 2021. DOI: <https://doi.org/10.1007/s13197-020-04645-6>.
- [11] M. Azizkhani, F. Tooryan, P. shohreh, R. Partovi, and M. H. Shahavi. “Evaluating the effect of Nanoemulsion of *Artemisia dracunculoides* Essential Oil on Expression of virulence genes in enterohemorrhagic *Escherichia coli*.”. *Journal of food science and technology (Iran)*, **17**:121–32, 2020. DOI: <https://doi.org/10.52547/fsct.17.106.121>.
- [12] H. Kazemeini, A. Azizian, and M. H. Shahavi. “Effect of Chitosan Nano-Gel/Emulsion Containing *Bunium Persicum* Essential Oil and Nisin as an Edible Biodegradable Coating on *Escherichia Coli* O157:H7 in Rainbow Trout Fillet.”. *Journal of Water and Environmental Nanotechnology*, **4**:343–9, 2019.
- [13] S-K. Yang, K. Yusoff, W. Thomas, R. Akseer, M. S. Alhosani, A. Abushelaibi, et al. “Lavender essential oil induces oxidative stress which modifies the bacterial membrane permeability of carbapenemase producing *Klebsiella pneumoniae*.”. *Scientific reports*, **10**:1–14, 2020.
- [14] H. Genc and S. Saritas. “The effects of lavender oil on the anxiety and vital signs of benign prostatic hyperplasia patients in preoperative period.”. *Explore*, **16**:116–22, 2020.
- [15] M. N. Abatari, M. R. S. Emami, M. Jahanshahi, and M. H. Shahavi. “Superporous pellicular  $\kappa$ -carrageenan-nickel composite beads; morphological, physical and hydrodynamics evaluation for expanded bed adsorption application.”. *Chemical Engineering Research and Design*, **125**:291–305, 2017.
- [16] M. H. Shahavi, M. Hosseini, M. Jahanshahi, and G. N. Darzi. “Optimization of encapsulated clove oil particle size with biodegradable shell using design expert methodology.”. *Pakistan Journal of Biotechnology*, **12**:149–60, 2015.
- [17] M. Jahanshahi, G. Najafpour, M. Ebrahimpour, S. Hajizadeh, and M. H. Shahavi. “Evaluation of hydrodynamic parameters of fluidized bed adsorption on purification of nano-bioproducts.”. *Physica Status Solidi C*, **6**:2199–206, 2009. DOI: <https://doi.org/10.1002/pssc.200881737>.
- [18] A. V. Samrot, U. Bisyarah, T. Kudaiyappan, F. Etel, and A. Abubakar. “Ficus *icyrata* plant gum derived polysaccharide based nanoparticles and its application.”. *Biocatalysis and Agricultural Biotechnology*, **31**:101871, 2021.
- [19] S. Davoodi, E. Oliaei, S. M. Davachi, I. Hejazi, J. Seyfi, B. S. Heidari, et al. “Preparation and characterization of interface-modified PLA/starch/PCL ternary blends using PLLA/triclosan antibacterial nanoparticles for medical applications.”. *Rsc Advances*, **6**:39870–82, 2016.
- [20] M. H. Shahavi, P. P. Selakjani, M. N. Abatari, P. Antov, and V. Savov. “Novel biodegradable poly (lactic acid)/wood leachate composites: investigation of antibacterial, mechanical, morphological, and thermal properties.”. *Polymers*, **14**:1227, 2022. DOI: <https://doi.org/10.3390/polym14061227>.
- [21] M. H. Shahavi, R. Esfilar, B. Golestani, M. Sadeghi Sadeghabad, and M. Biglaryan. “Comparative study of seven agricultural wastes for renewable heat and power generation using integrated gasification combined cycle based on energy and exergy analyses.”. *Fuel*, **317**:123430, 2022. DOI: <https://doi.org/10.1016/j.fuel.2022.123430>.
- [22] S. J. Owonubi, E. Mukwevho, B. A. Aderibigbe, N. Revaprasadu, and E. R. Sadiku. “Cytotoxicity and in vitro evaluation of whey protein-based hydrogels for diabetes mellitus treatment.”. *International Journal of Industrial Chemistry*, **10**:213–23, 2019. DOI: <https://doi.org/10.1007/s40090-019-0185-4>.
- [23] M. Hosseini, M. H. Shahavi, and A. Yakhkeshi. “AC & DC-currents for separation of nano-particles by external electric field.”. *Asian Journal of Chemistry*, **24**:181–4, 2012.

- [24] M. Shahavi, M. Jahanshahi, G. Najafpour, M. Ebrahimpour, and A. Hosenian. "Expanded bed adsorption of biomolecules by NBG contactor: Experimental and mathematical investigation." *World Applied Sciences Journal*, **13**:181–7, 2011.
- [25] R. Deng, C. Selomulya, P. Wu, M. W. Woo, X. Wu, and X. D. Chen. "A soft tubular model reactor based on the bionics of a small intestine – Starch hydrolysis." *Chemical Engineering Research and Design*, **112**:146–54, 2016. DOI: <https://doi.org/10.1016/j.cherd.2016.06.005>.
- [26] F. Ortega, V. B. Arce, and M. A. Garcia. "Nanocomposite starch-based films containing silver nanoparticles synthesized with lemon juice as reducing and stabilizing agent." *Carbohydrate polymers*, **252**:117208, 2021.
- [27] S. Kumari, B. S. Yadav, and R. B. Yadav. "Synthesis and modification approaches for starch nanoparticles for their emerging food industrial applications: A review." *Food Research International*, **128**:108765, 2020.
- [28] A Soleymani Lashkenrai, M. Najafi, M. Peyravi, M. Jahanshahi, M. T. H. Mosavian, A. Amiri, et al. "Direct filtration procedure to attain antibacterial TFC membrane: A facile developing route of membrane surface properties and fouling resistance." *Chemical Engineering Research and Design*, **149**:158–68, 2019. DOI: <https://doi.org/10.1016/j.cherd.2019.07.003>.
- [29] N. Lammari, O. Louaer, A. H. Meniai, and A. Elaisari. "Encapsulation of essential oils via nanoprecipitation process: Overview, progress, challenges and prospects." *Pharmaceutics*, **12**:431, 2020.
- [30] A. Sirivat and N. Paradee. "Facile synthesis of gelatin-coated Fe<sub>3</sub>O<sub>4</sub> nanoparticle: Effect of pH in single-step co-precipitation for cancer drug loading." *Materials & Design*, **181**:107942, 2019.
- [31] S. Tabasum, M. Younas, M. A. Zaeem, I. Majeed, M. Majeed, A. Noreen, et al. "A review on blending of corn starch with natural and synthetic polymers, and inorganic nanoparticles with mathematical modeling." *International journal of biological macromolecules*, **122**:969–96, 2019.
- [32] Q. Su, Y. Wang, X. Zhao, H. Wang, Z. Wang, N. Wang, et al. "Functionalized nano-starch prepared by surface-initiated atom transfer radical polymerization and quaternization." *Carbohydrate polymers*, **229**:115390, 2020.
- [33] V. K. Rai, P. Sinha, K. S. Yadav, A. Shukla, A. Saxena, D. U. Bawankule, et al. "Anti-psoriatic effect of Lavandula angustifolia essential oil and its major components linalool and linalyl acetate." *Journal of Ethnopharmacology*, **261**:113127, 2020.
- [34] H. Dong, Q. Zhang, J. Gao, L. Chen, and T. Vasanthan. "Comparison of morphology and rheology of starch nanoparticles prepared from pulse and cereal starches by rapid antisolvent nanoprecipitation." *Food Hydrocolloids*, :106828, 2021.
- [35] R. Mofidian, A. Barati, M. Jahanshahi, and M. H. Shahavi. "Fabrication of novel agarose–nickel bilayer composite for purification of protein nanoparticles in expanded bed adsorption column." *Chemical Engineering Research and Design*, **159**:291–9, 2020. DOI: <https://doi.org/10.1016/j.cherd.2020.03.024>.
- [36] R. Mofidian, A. Barati, M. Jahanshahi, and M. H. Shahavi. "Generation process and performance evaluation of engineered microsphere agarose adsorbent for application in fluidized-bed systems." *International Journal of Engineering*, **33**:1450–8, 2020. DOI: <https://doi.org/10.5829/ije.2020.33.08b.02>.
- [37] Y. Qin, C. Liu, S. Jiang, L. Xiong, and Q. Sun. "Characterization of starch nanoparticles prepared by nanoprecipitation: Influence of amylose content and starch type." *Industrial Crops and Products*, **87**:182–90, 2016.
- [38] B. Momenpoor, F. Danafar, and F. Bakhtiari. "Size controlled preparation of starch nanoparticles from wheat through precipitation at low temperature." *Journal of Nano Research: Trans Tech Publ*, :131–41, 2019.
- [39] M. Jahanshahi and M. H. Shahavi. "Chapter 17 - Advanced Downstream Processing in Biotechnology. In: Najafpour GD, editor. Biochemical Engineering and Biotechnology (Second Edition). Amsterdam: Elsevier." :495–526., 2015.
- [40] M. H. Shahavi, M. Hosseini, M. Jahanshahi, R. L. Meyer, and G. Najafpour Darzi. "Evaluation of critical parameters for preparation of stable clove oil nanoemulsion." *Arabian Journal of Chemistry*, **12**:3225–30, 2019. DOI: <https://doi.org/10.1016/j.arabjc.2015.08.024>.
- [41] J. Perez Quinones, O. Bruggemann, J. Kjemis, M. H. Shahavi, and C. Peniche Covas. "Novel brassinosteroid-modified polyethylene glycol micelles for controlled release of agrochemicals." *Journal of agricultural and food chemistry*, **66**:1612–9, 2018. DOI: <https://doi.org/10.1021/acs.jafc.7b05019>.
- [42] R. Mofidian, A. Barati, M. Jahanshahi, and M. H. Shahavi. "Optimization on thermal treatment synthesis of lactoferrin nanoparticles via Taguchi design method." *SN Applied Sciences*, **1**:1339, 2019. DOI: <https://doi.org/10.1007/s42452-019-1353-z>.
- [43] Z Sefrou and N-E. Belkhouche. "Cloud point extraction of La(III) by C13E10 non-ionic surfactant: Statistical refinement of experimental optimization by L9 Taguchi's design." *Chemical Engineering Research and Design*, **153**:819–28, 2020. DOI: <https://doi.org/10.1016/j.cherd.2019.11.027>.

- [44] M. H. Shahavi, M. Hosseini, M. Jahanshahi, R. L. Meyer, and G. N. Darzi. "Clove oil nanoemulsion as an effective antibacterial agent: Taguchi optimization method. ". *Desalination and Water Treatment*, **57**:18379–90, 2016. DOI: <https://doi.org/10.1080/19443994.2015.1092893>.
- [45] K. Singh and I. Sultan. "Parameters optimization for sustainable machining by using Taguchi method. ". *Materials Today: Proceedings*, **18**:4217–26, 2019.
- [46] S. F. Chin, S. C. Pang, and S. H. Tay. "Size controlled synthesis of starch nanoparticles by a simple nano-precipitation method. ". *Carbohydrate Polymers*, **86**: 1817–9, 2011.
- [47] h. Xiao, F. Yang, Q Lin, Q. Zhang, L Zhang, S. Sun, et al. "Preparation and characterization of broken-rice starch nanoparticles with different sizes.". *International Journal of Biological Macromolecules*, **160**: 437–45, 2020.
- [48] C. Qiu, R. Chang, J. Yang, S. Ge, L. Xiong, M. Zhao, et al. "Preparation and characterization of essential oil-loaded starch nanoparticles formed by short glucan chains.". *Food Chemistry*, **221**:1426–33, 2017. DOI: <https://doi.org/10.1016/j.foodchem.2016.11.009>.
- [49] O. P. Troncoso and F. G. Torres. "Non-conventional starch nanoparticles for drug delivery applications.". *Medical Devices & Sensors*, **3**:e10111, 2020.
- [50] A. Jain, F. Ahmad, D. Gola, A. Malik, N. Chauhan, P. Dey, et al. "Multi dye degradation and antibacterial potential of Papaya leaf derived silver nanoparticles.". *Environmental Nanotechnology, Monitoring & Management*, :14, 2020.
- [51] M. Khalili, A. Razmjou, R. Shafiei, M. H. Shahavi, M-C Li, and Y. Orooji. "High durability of food due to the flow cytometry proved antibacterial and antifouling properties of TiO<sub>2</sub> decorated nanocomposite films.". *Food and Chemical Toxicology*, **168**:113291, 2022. DOI: <https://doi.org/10.1016/j.fct.2022.113291>.
- [52] M. H. Damani, R. Partovi, M. H. Shahavi, and M. Azizkhani. " Nanoemulsions of Trachyspermum copiticum, Mentha pulegium and Satureja hortensis essential oils: formulation, physicochemical properties, antimicrobial and antioxidant efficiency.". *Journal of Food Measurement and Characterization*, **16**:1807–19, 2022.
- [53] N. S. Ismail and S. C. Gopinath. "Enhanced antibacterial effect by antibiotic loaded starch nanoparticle.". *Journal of the Association of Arab Universities for Basic and Applied Sciences*, **24**:136–40, 2017.